

Regulation of membrane scission in yeast endocytosis

Deepikaa Menon¹ and Marko Kaksonen^{1*}

*For correspondence:

Marko.Kaksonen@unige.ch

¹Department of Biochemistry, University of Geneva, Geneva, Switzerland

Abstract

Introduction

In Clathrin-mediated endocytosis, a flat plasma membrane is pulled into a tubular invagination that eventually forms a vesicle. Forces that drive the transition from invagination to spherical vesicle in mammalian cells are provided by constriction of the GTPase Dynamin. Dynamin is now known to act in concert with the crescent-shaped N-BAR proteins Endophilin and Amphiphysin (ref. Dynamin papers). Proline-rich motifs on the Dynamin. In yeast cells, what causes membrane scission is unclear, although the yeast N-BAR protein complex Rvs has been identified as an important component of the scission module. In yeast, the Amphiphysin and Endophilin homologue Rvs is a heterodimeric complex composed of Rvs161 and Rvs167 (Friesen et al., 2006). Deletion of Rvs reduces scission efficiency by nearly 30% and reduces the invagination lengths at which scission occurs (ref Marko, wanda). Apart from a canonical N-BAR domain which forms a crescent-shaped structure, Rvs167 has a Glycine-Proline-Alanine rich (GPA) region and a C-terminal SH3 domain. Rvs161 and Rvs167 N-BAR domains are 42% similar, and 21% identical, but are not interchangeable (Sivadon, Crouzet and Aigle, 1997). The GPA region is thought to act as a linker with no known other function, while loss of the SH3 domain affects budding pattern and actin morphology. Most Rvs deletion phenotypes can however, be rescued by expression of the BAR domain alone (Sivadon, Crouzet and Aigle, 1997), suggesting that the BAR domains are the main functional unit of the Rvs complex. Homology modelling has shown that the BAR domain of Rvs167 is similar to Amphiphysin and Endophilin (Youn et al., 2010), and is therefore likely to function similarly to the mammalian homologues. In keeping with this theory, Rvs has been shown to tubulate liposomes in vitro (Youn et al., 2010). The Rvs complex arrives at endocytic sites in the last stage of the endocytosis, and disassembles rapidly at the time of membrane scission (Picco et al., 2015), consistent with a role in membrane scission. While it is known to be involved in the last stages of endocytosis, a mechanistic understanding of the influence of Rvs on scission however, remains incomplete. u89

We used quantitative live-cell imaging and genetic manipulation in *S.cereviciae* to investigate the influence of Rvs and several Rvs interacting proteins that have been suggested to have a role in scission. We found that arrival of Rvs to endocytic sites is timed by interaction of its BAR domain with a specific membrane curvature. The Rvs167 SH3 domain affects localization efficiency of the Rvs complex and also influences invagination dynamics. This indicates that both BAR and SH3 domains are important for the role of Rvs as a regulator of scission. We tested current models of membrane scission, and find that deleting yeast synaptojanins or dynamin does not change scission dynamics. Interfacial forces at lipid boundaries are therefore unlikely to be sufficient for scission, and forces exerted by dynamin are not required. Furthermore, invagination length is insensitive to overexpression of Rvs, suggesting that the recently proposed mechanism of BAR-induced protein friction on the membrane is not likely to drive scission. We propose that recruitment of Rvs BAR

43 domains prevents scission and allows invaginations to grow by stabilizing them. We also propose
 44 that vesicle formation is dependent on forces exerted by a different module of the endocytic
 45 pathway, the actin network. Preventing premature membrane scission via BAR interaction could
 46 allow invaginations to grow to a particular length and accumulate enough forces within the actin
 47 network to reliably cut the membrane.

48 Results

49 Removal of Rvs167, not Vps1, results in reduced coat movement

50 The yeast Dynamin-like protein Vps1 does not contain the canonical Proline Rich Domain, which
 51 in mammalian cells is required for recruitment to endocytic sites (ref). It is however, reportedly
 52 recruited to and interacts with endocytic proteins (refAyscough, Yu, 2004; Nannapaneni et al., 2010;
 53 Goud Gadila et al., 2017). Vps1 tagged both N- and C-terminally with GFP constructs failed to
 54 co-localize with endocytic protein Abp1 in our hands (Fig.1 supplement).

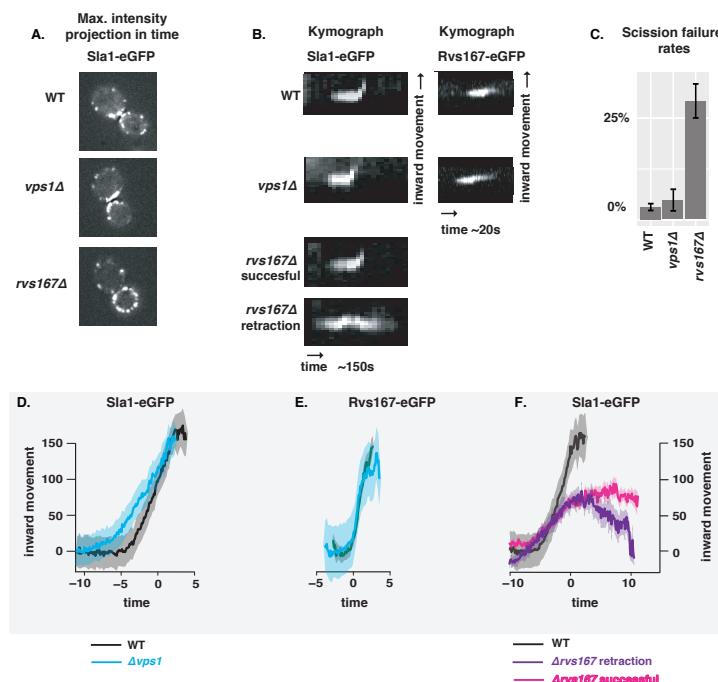


Figure 1. A: Maximum projection in time of WT, *vps1Δ*, and *rvs167Δ* cells expressing Sla1-eGFP. B: Representative kymographs of Sla1-eGFP and Rvs167-eGFP patches in these cells. C: Histogram of retraction rates in WT, *vps1Δ*, and *rvs167Δ* cells, determined from tracking Sla1-eGFP in these cells. Error bars are standard deviation from two data sets, $p < 0.001 = *$. D: Averaged centroid positions of Sla1-eGFP (D, F) in WT and *vps1Δ* cells. E: Averaged Rvs167-eGFP position in the same strains. F: Averaged Sla1-eGFP position in WT and successful and retracted Sla1-eGFP positions in *rvs167Δ* cells. All averaged positions are aligned in time to begin inward movement at the same time=0(seconds), and aligned in space to a starting position = 0 (nm)

55 To test whether absence of Vps1 influences scission, endocytic dynamics are observed in cells
 56 lacking Vps1 and compared against wild-type (WT) cells (Fig.1a-f). Vps1 deletion is confirmed by
 57 sequencing the open reading frame, and these cells show the growth phenotype at 37°C (Fig.1,
 58 supplement2) recorded in other work (ref. ayscough). In Fig.1c, rates of retraction of the membrane
 59 in *vps1Δ* and WT cells is quantified. Membrane retraction, that is, inward movement and subsequent
 60 retraction of the invaginated membrane back towards the cell wall is a scission-specific phenotype
 61 (ref.Marko). Sla1 is an endocytic coat protein that acts as a marker for membrane movement.
 62 Upon actin polymerization, the endocytic coat is pulled along with the membrane as it invaginates
 63 (ref.Skrzyn?), and thus Sla1 acts as a proxy for the behaviour of the plasma membrane. We

64 endogenously tagged Sla1 at the C-terminus with eGFP in WT and *rvs167Δ* cells (Fig.1a), and tracked
65 the dynamics. Retraction rates do not increase in *vps1Δ* cells compared to the WT (Fig.1c).

66
67

68 In order to study the total inward movement of the coat, and therefore the depth of the endocytic
69 invagination, the averaged centroid trajectory of Sla1-eGFP (ref. Picco, eLife 2015) is tracked in 50
70 endocytic sites in *vps1Δ* and WT cells (Fig.1d). In brief, yeast cells expressing fluorescently-tagged
71 endocytic proteins are imaged at the equatorial plane. Since membrane invagination progresses
72 perpendicularly to the plane of the plasma membrane, proteins that move into the cytoplasm
73 during invagination do so in the imaging plane. Centroids of 40-50 Sla1 patches- each patch being
74 an endocytic site- are tracked in time and averaged. This provides an average centroid that can
75 be followed with high spatial and temporal resolution. When different endocytic proteins are
76 simultaneously imaged with Actin Binding Protein Abp1, Abp1 provides a frame of reference to
77 which all the other proteins can be aligned. Abp1 is used because it is abundant at endocytic
78 sites and therefore easily imaged. Time=0 is established as the peak of the Abp1 fluorescence
79 intensity in respective co-tagged strains strains. Abp1 fluorescent intensity maxima in wild-type
80 cells is concomitant with the peak of Rvs167 fluorescent intensity and is time window in which
81 scission occurs (ref2andrea, refwanda). Centroid movement of Sla1-eGFP in WT cells is linear to
82 about 140nm. Sla1 movement in *vps1Δ* cells has the same magnitude of movement (Fig1d). In spite
83 of slight differences in the rates of movement, the total inward movement- and so the depth of
84 endocytic invagination- does not change.

85
86

87 Centroid tracking has shown that the number of molecules of Rvs167 peaks at the time of
88 scission, and is followed by a rapid loss of fluorescent intensity, simultaneous with a sharp jump
89 of the centroid into the cytoplasm (ref.Andrea). This jump, also seen in Rvs167-GFP kymographs
90 (Fig.1b), is interpreted as loss of protein on the membrane tube, causing an apparent spatial jump to
91 the protein localized at the base of the newly formed vesicle. Kymographs of Rvs167-GFP (Fig.1b), as
92 well as Rvs167 centroid tracking (Fig.1e) in Vps1 deleted cells show the same jump. Sla1 and Rvs167
93 behaviour in *vps1Δ* cells indicate that loss of Vps1 does not influence the depth of membrane
94 invagination or scission dynamics.

95

96 Since removal of the Rvs complex is known to increase the retraction rate at endocytic sites,
97 involvement of these proteins in the scission process was investigated further. Rvs161 and Rvs167
98 form dimers (ref.Dominik), so deletion of Rvs167 effectively removes both proteins from endocytic
99 sites. We quantified the effect of deletion of Rvs167 on membrane invagination (Fig.1a-c). 27% of
100 Sla1 patches that begin to form invaginations move inward and then retract in *rvs167Δ* cells (Fig.1c),
101 consistent with retraction rates measured in other experiments (Kaksonen, Toret and Drubin, 2005),
102 and suggesting failed scission in these 27% of endocytic events. Coat movement of the retractions
103 and of successful endocytic events were quantified (Fig.1f) as described in Picco et. al, 2015. Sla1
104 centroid movement in both successful and retracting endocytic events in *rvs167Δ* cells and WT
105 look similar up to about 60nm (Fig.1f). In successful endocytic events, Sla1-egfp signal is then lost,
106 similar to WT cells, and Abp1 intensity drops (Fig.1supplement), indicating that scission occurs at
107 invagination lengths between 60 -80 nm. That membrane scission occurs at shorter invagination
108 lengths than in WT is corroborated by the smaller vesicles formed in *rvs167Δ* cells by Correlative
109 light and electron microscopy (CLEM) (Kukulski et al., 2012). In retraction events, the Sla1 centroid
110 moves back towards its original position. CLEM has also shown that Rvs167 localizes to endocytic
111 sites after the invaginations are about 60nm long (Kukulski et al., 2012). Sla1 movement in *rvs167Δ*
112 indicates therefore that membrane invagination is unaffected till Rvs is supposed to arrive.

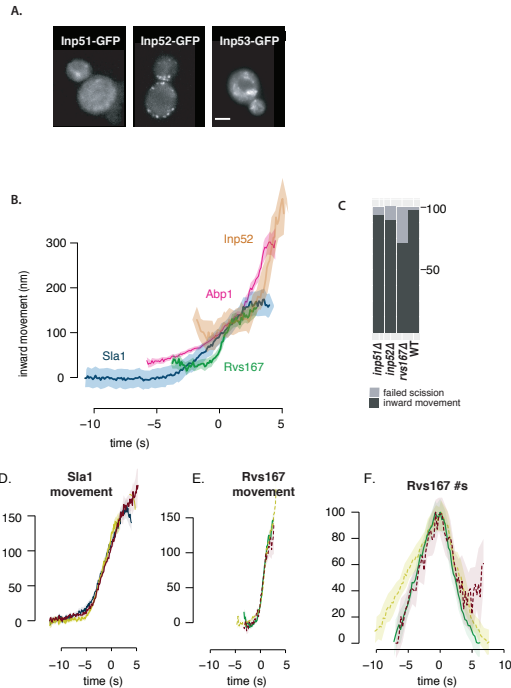


Figure 2. A half-columnwidth image using wrapfigure, to be used sparingly. Note that using a wrap figure before a sectional heading, near other floats or page boundaries is not recommended, as it may cause interesting layout issues. Use the optional argument to wrapfigure to control how many lines of text should be set half-width alongside it.

113 **Synaptojanins likely influence vesicle uncoating, but not scission dynamics.**

114 There are three Synaptojanin-like proteins in budding yeast: Inp51, Inp52, and Inp53 (Fig2a). Inp51-
 115 eGFP exhibits a diffuse cytoplasmic signal, and Inp53 localizes to patches within the cytoplasm-
 116 cellular localization that is consistent with involvement in trans-Golgi signalling (refGolgi)- Inp53
 117 was not investigated further. Inp52-eGFP localizes to cortical actin patches that are endocytic sites
 118 (Fig2 supplement). Spatial and temporal alignment with Sla1 and Rvs167 shows that Inp52 protein
 119 molecules arrive in the late scission stage, and localizes to the bud tip, consistent with a role in
 120 membrane scission (Fig.2b).

121 Inp51 and Inp52 were tested as potential candidates for scission regulators. Sla1-eGFP and
 122 Rvs167-eGFP in cells with either Inp51 or Inp52 deleted were studied. Retraction events do not
 123 significantly increase compared to the WT in either *inp51Δ* or *inp52Δ* cells (Fig2c). Magnitude and
 124 speed of coat movement in *inp51Δ* is the same as the WT (Fig2.d). In *inp52Δ* cells, coat movement
 125 also has the magnitude and speed as WT, but Sla1-eGFP signal is persistent after membrane scission
 126 (Fig.2d). Similarly, although Rvs167 inward movement looks the similar (Fig2e), disassembly has a
 127 delay, while the assembly is similar to WT (Fig2f). Assembly of Rvs167 has a delay in *inp51Δ* cells.
 128 The magnitude of the inward movement of both Sla1 and Rvs167 in cells containing either deletion
 129 are the same as in WT, while assembly and disassembly dynamics of Rvs167 is changed.

130 **Rvs BAR domains recognize membrane curvature in-vivo**

131 The interaction between Rvs167 and membrane curvature *in vivo* has not so far been tested. In
 132 order to do so, we deleted the SH3 domain of Rvs167 leaving the N-terminal BAR region (henceforth
 133 BAR-GPA) and observed the localization of full-length Rvs167 and BAR-GPA (Fig3a). The GPA region
 134 is a disordered region that has no previously reported function and was retained to ensure proper
 135 folding and function of the BAR domain. Endogenously tagged Rvs167-eGFP and BAR-GPA-eGFP
 136 colocalization with Abp1-mCherry in WT and *sla2Δ* cells are compared (Fig3b). Sla2 acts as the

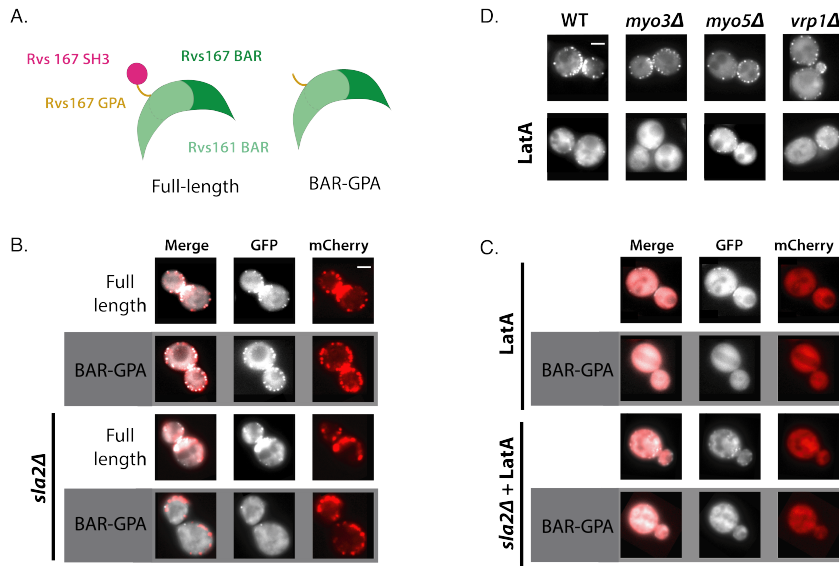


Figure 3. A half-columnwidth image using wrapfigure, to be used sparingly. Note that using a wrap figure before a sectional heading, near other floats or page boundaries is not recommended, as it may cause interesting layout issues. Use the optional argument to wrapfigure to control how many lines of text should be set half-width alongside it.

137 molecular linker between forces exerted by the actin network and the plasma membrane (ref.
 138 Skuzny). *sla2Δ* cells therefore contain a polymerizing actin network at endocytic patches, but the
 139 membrane remains flat and endocytosis fails. In these cells, the full-length Rvs167 protein co-
 140 localizes with Abp1-mCherry, indicating that it is recruited to endocytic sites (Fig3b). BAR-GPA-eGFP
 141 localization is removed, except for rare transient patches that do not co-localize with Abp1-mCherry,
 142 indicating that in the absence of membrane curvature, the BAR domains cannot localize to endocytic
 143 sites (Fig3b, *sla2Δ*).

144 **SH3 domains are likely recruited by Myosin 3**

145 SH3 domains have been shown to interact with several proteins in the actin module of endocytosis.
 146 Type I myosins Myo3 and Myo5, and Vrp1 have genetic or physical interactions with Rvs167 SH3
 147 domains (Lila and Drubin, 1997; Colwill et al., 1999; Madania et al., 1999; Liu et al., 2009). We tested
 148 the interaction between these proteins and the Rvs167-SH3 region by studying the localization of
 149 full-length Rvs167 in cells with one of these proteins deleted, and treated with LatA to reproduce
 150 the situation in which BAR-curvature interaction is removed, and SH3 interaction remains. Deletion
 151 of neither Vrp1 nor Myo5 in combination with LatA treatment removes the localization of Rvs167.
 152 Deletion of Myo3 with LatA treatment removes localization of Rvs167.

153 **what about the differences in myo5 and myo3 number...**

154 **Loss of Rvs167 SH3 domain affects coat and actin dynamics**

155 In order to further probe the contribution of the Rvs167 SH3 domain to endocytosis, we compared
 156 dynamics of Sla1, as well as Rvs167 and BAR-GPA centroids (Fig4a). Movement of Sla1 centroid is
 157 reduced in BAR-GPA cells (Fig4a). Both full length Rvs167 and BAR-GPA however, arrive at endocytic
 158 coats when Sla1 centroid is about 30nm away from the initial position (Fig1a, red line to the y axis).
 159 Tubular invaginations are formed in BAR cells, and qualitatively resemble that in WT cells, as seen by
 160 CLEM (Fig.4 supplement). The inward jump of BAR-GPA is less than that of full-length Rvs167 (Fig.4b).
 161 Recruitment of BAR is reduced to half that of Rvs167 (Fig4c), although cytoplasmic concentration of
 162 Rvs167 and BAR are not different (Fig4 supplement). We also quantified the number of Abp1 and
 163 Rvs molecules recruited to endocytic sites (Fig4b). Abp1 disassembly is slowed down in BAR-GPA

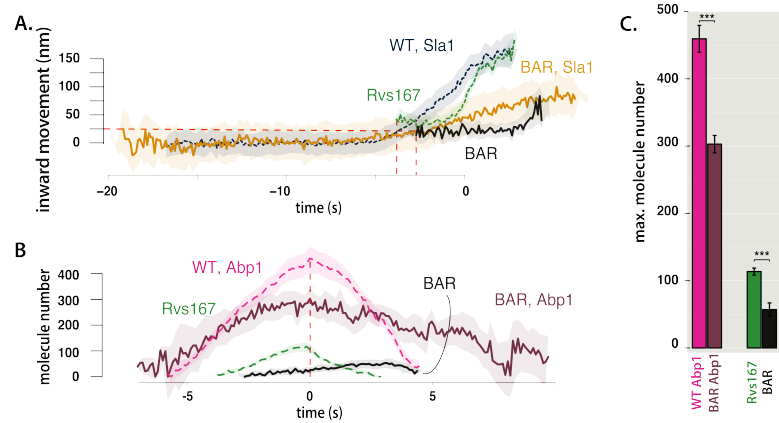


Figure 4. A half-columnwidth image using wrapfigure, to be used sparingly. Note that using a wrapfigure before a sectional heading, near other floats or page boundaries is not recommended, as it may cause interesting layout issues. Use the optional argument to wrapfigure to control how many lines of text should be set half-width alongside it.

164 cells compared to WT (Fig4b), and recruitment is reduced to 50% of WT recruitment (Fig.4c), likely
165 indication disruption of actin network assembly.

166 **N-helix and GPA domains do not contribute to recruitment of Rvs or membrane 167 movement**

168 Etiam euismod. Fusce facilisis lacinia dui. Suspendisse potenti. In mi erat, cursus id, nonummy
169 sed, ullamcorper eget, sapien. Praesent pretium, magna in eleifend egestas, pede pede pretium
170 lorem, quis consectetur tortor sapien facilisis magna. Mauris quis magna varius nulla scelerisque
171 imperdiet. Aliquam non quam. Aliquam porttitor quam a lacus. Praesent vel arcu ut tortor cursus
172 volutpat. In vitae pede quis diam bibendum placerat. Fusce elementum convallis neque. Sed dolor
173 orci, scelerisque ac, dapibus nec, ultricies ut, mi. Duis nec dui quis leo sagittis commodo.

174 **Reduced BAR domain recruitment corresponds to reduced membrane movement**

175 Decreased Sla1 movement in BAR-GPA cells (Fig4a) can be explained by loss of some interaction
176 mediated by the SH3 domain, or because the BAR-GPA mutant is recruited in smaller numbers to
177 endocytic sites. To check whether increasing the recruitment of the Rvs complex alone can rescue
178 reduced Sla1 movement, Rvs167 and Rvs161 genes were duplicated endogenously (ref Huber) in
179 diploid and haploid yeast cells. Diploid cells are thus generated containing either 4 copies of both
180 Rvs genes (by gene duplication), 2 copies of each gene (WT diploid), or 1 copy (by deleting one copy
181 of Rvs167 and Rvs161). In diploid cells (Fig5a-c), amount of Rvs167 recruited to sites increases with
182 gene copy number (Fig5c). Adding excess Rvs to endocytic sites in the 4x case does not change
183 the rate or total inward movement of Sla1, or of Rvs167. In the case of 1x Rvs, Sla1 movement is
184 slightly reduced after 100nm (Fig5a). Magnitude of Rvs167 inward movement is unchanged, but the
185 Rvs167-eGFP signal is lost immediately after the inward movement, unlike in the 4x and 2x cases. In
186 haploid cells, increasing the number of Rvs167 and Rvs161 genes results in increased recruitment
187 of Rvs167 to about 1.6 times the WT amount (Fig5f,h). Sla1 dynamics however, remains the same
188 as in the WT(Fig5d). Duplicating the BAR-GPA domain alone rescues the loss of Sla1 movement
189 in the 1x BAR-GPA, as well the inward jump of BAR-GPA itself (Fig5d,e). We measured the total
190 number of Abp1 molecules at endocytic sites for different strains (Fig5g,h), and found that higher
191 Abp1 numbers corresponds to larger Sla1 centroid movement. Total Abp1 numbers recruited are
192 reduced for 1xBAR and rvs167Δ strains (Fig5g,h), suggesting a correlation between the maximum
193 number of Abp1 recruited and total invagination length.

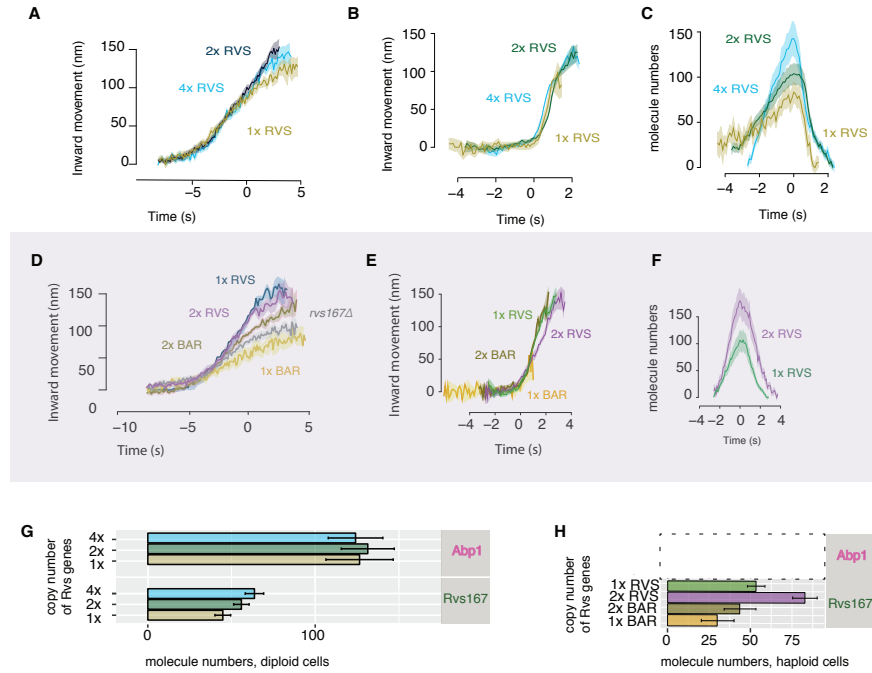


Figure 5. A half-columnwidth image using wrapfigure, to be used sparingly. Note that using a wrapfigure before a sectional heading, near other floats or page boundaries is not recommended, as it may cause interesting layout issues. Use the optional argument to wrapfigure to control how many lines of text should be set half-width alongside it.

194 Discussion

195 Recruitment and function of the Rvs complex in has been explored in this work, as well as several
 196 models for how membrane scission could be effected in yeast endocytosis. We propose that
 197 Rvs is recruited to endocytic sites by interactions between the Rvs BAR domains and invaginated
 198 membrane, and that SH3 domain mediated protein-protein interactions are required for efficient
 199 recruitment of Rvs to sites. Arrival of Rvs on membrane tube scaffolds the membrane and prevents
 200 premature membrane scission. Effective scaffolding depends on recruitment of a critical number
 201 of Rvs molecules. Rvs is a relatively short-lived protein at endocytic sites. It is recruited only once
 202 membrane tube is formed (Kaksonen, Toret and Drubin, 2005; Kukulski et al., 2012; Picco et al.,
 203 2015). FCS measurements (Boeke et al., 2014) have shown that the cytosolic concentrations of
 204 Rvs167 and Rvs161 are high (354nM and 721nM respectively) compared to other endocytic proteins
 205 like Las17, Vrp1, Myo3, and Myo5 (80-240nM). In spite of this, relatively few numbers of Rvs are
 206 recruited to endocytic sites, suggesting that recruitment is tightly regulated. In the case of Rvs, both
 207 timing and efficiency appear crucial to its function, the question is what confers both.

208 **BAR domains sense *in vivo* membrane curvature and time recruitment of Rvs**

209 The curved structure of BAR dimers (Peter et al., 2004; Mim et al., 2012) has suggested that Rvs
 210 is recruited by its preference for some membrane shapes over others, supported by its arrival at
 211 curved membrane tubes. In the absence of membrane curvature, in *sla2Δ* cells, the BAR domain
 212 alone does not localize to cortical patches (Fig.3b,c). This demonstrates for the first time that the
 213 BAR domain does indeed sense and requires membrane curvature to localize to cortical patches.
 214 Work on BAR domains have proposed that electrostatic interactions at the concave surface and
 215 tips of the BAR domain structure mediate membrane binding (Qualmann, Koch and Kessels, 2011).
 216 Mutations in these lipid-binding surfaces would clarify the interaction with underlying lipids, and

217 test if Rvs relies on similar interactions. BAR is able to localize to endocytic sites, and has a similar
218 lifetime in WT cells (Fig4b). However, time alignment with Abp1 shows that there is a delay in the
219 recruitment of BAR-GPA compared to Abp1 arrival, compared to full-length Rvd167 (Fig4c). The
220 delayed recruitment occurs because the invagination takes longer to reach a particular length: Sla1
221 moves inwards at a slower rate in BAR cells, and it takes longer for the membrane in BAR-GPA cells
222 to reach the same length as Rvs167. Rvs167 arrives in BAR cells when Sla1 has moved inwards
223 25-30nm (dashed red lines in Fig.4a), which is also the distance Sla1 has moved when Rvs167 arrives
224 in WT. By the time Sla1 has moved this distance, the membrane is already tubular (Kukulski et
225 al., 2012; Picco et al., 2015), consistent with Rvs arrival at invaginated tubes. This suggests Rvs
226 recruitment is timed to specific membrane invagination length- therefore to a specific membrane
227 curvature- and that this timing is provided by the BAR domain.

228 **SH3 domains allow efficient and actin independent recruitment**

229 Rvs167 in BAR cells accumulates to about half the WT number (Fig.3c), even though the same cyto-
230 plasmic concentration is measured (supplement Fig3?), indicating that the SH3 domain increases
231 the efficiency of recruitment of Rvs. In *sla2Δ* cells, full-length Rvs can assemble on the membrane
232 (Fig.3b,c). Since BAR domains alone do not localize to patches in *sla2Δ* cells, full-length localization
233 must be mediated by the SH3 domain, supporting a role for the SH3 domain in increasing
234 recruitment of Rvs by clustering protein molecules. That full-length Rvs167 is able to assemble and
235 disassemble at cortical patches in *sla2Δ* cells without the curvature- dependent interaction of the
236 BAR domain (Fig.3b,c) indicates that the SH3 domain is able to mediate both the recruitment and
237 the disassembly of Rvs at the endocytic site. In *sla2Δ* cells treated with LatA (Fig.3c), actin-based
238 membrane curvature is inhibited, and the actin patch proteins are removed from the plasma mem-
239 brane. Full-length Rvs167 in these cells still shows transient localizations at the plasma membrane.
240 In *sla2Δ* cells treated with LatA, the localization of BAR is lost. This suggests that localization of the
241 full-length Rvs167 in LatA treated cells is dependent on an SH3 domain interaction, and that this is
242 independent of both actin and membrane curvature.

243 In WT cells, the Abp1 and Rvs167 fluorescent intensities reach maxima concomitantly (Fig4b),
244 and the consequent decay of both also coincide. Coincident disassembly indicates that upon vesicle
245 scission, the actin network is immediately disassembled. Membrane scission essentially occurs
246 around the intensity peak of the two proteins. This coincident peak is lost in BAR-GPA cells: BAR-
247 GPA-eGFP in these cells peaks several seconds after Abp1 intensity starts to drop, and the decay of
248 Abp1 is prolonged, taking nearly double the time as in WT. The number of Abp1 molecules recruited
249 is decreased to about two thirds the WT number. Although it is not clear what the decoupling of
250 Abp1 and Rvs peaks means, the changes in Abp1 dynamics suggests a strong disruption of the actin
251 network dynamics. SH3 domains are known to interact with components of the actin network like
252 Abp1 and Las17 (Lila and Drubin, 1997, Madania et al., 1999), but study of other components of
253 the actin machinery will be required to understand how exactly loss of the SH3 has changed the
254 progression of endocytosis.

255 SH3 interaction with an endocytic binding partner likely help recruit Rvs to endocytic sites. Many
256 such interaction partners have been proposed. Abp1 interaction with the Rvs167 SH3 domain
257 has been shown (Lila and Drubin, 1997; Colwill et al., 1999), as has one with WASP protein Las17
258 (Madania et al., 1999; Liu et al., 2009), yeast Calmodulin Cmd1 (Myers et al., 2016), type I myosins
259 (Geli et al., 2000), and Vrp1 (Lila and Drubin, 1997). All of these suggested binding partners localize
260 to the base of the invagination (Yidi Sun, 2006; Picco et al., 2015), and do not follow the invaginating
261 membrane into the cytoplasm. The SH3 interaction partner is likely Myo3 (Fig3d), and SH3 domains
262 interact with the endocytic network at the base of the invagination. Centroid tracking however,
263 suggests that Rvs is accumulated all over the membrane tube. If Rvs was recruited to the base and
264 pulled up as the invagination grows, the centroid would move continuously upwards rather than
265 remain relatively non-motile before the jump at scission time. It is possible that the SH3 initially
266 helps cluster near the base, and as the membrane invaginations grow longer, BAR-membrane

267 interactions dominate.

268 **Accumulation of Rvs on membrane invagination**

269 When ploidy is doubled from haploid to diploid yeast cells, we could expect that double the protein
270 amount is expressed and recruited, but it does not appear so. The amount of Rvs recruited in
271 WT haploid and diploids remains about the same, and cytoplasmic signal is similar (Fig.5, Fig5
272 supplement). This invariance between accumulated protein in haploids and diploids shows that Rvs
273 recruitment is not determined by the number of alleles of Rvs. Haploid and diploid cells appear
274 to tune the amount of Rvs recruitment to get a specific amount to endocytic sites. WT diploids
275 (2xd) contain two copies each of RVS161 and RVS167 genes. Rvs duplicated diploids, which contain
276 four copies each of RVS167 and RVS161 (4xd) could be expected to express and recruit to sites
277 twice the amount of Rvs as 2xd. However, compared to 2xd, cytoplasmic signal in 4xd increases
278 by 1.6x and recruitment of Rvs167 to endocytic sites increases only by 1.4x. Doubling the gene
279 copy number increases, but does not double protein expression or recruitment in the case of
280 Rvs. Similarly, duplicating Rvs genes in haploid cells results in an increase in number of molecules
281 recruited, but not in doubling (1xh, 2xh). Although the rate of adding Rvs is different in haploids and
282 diploids, in both cases, it increases by gene copy number (yellow line in Fig.4.2). Cytoplasmic protein
283 concentration is increased when gene copy number is increased, and recruitment to endocytic
284 sites is increased by the increase in cytoplasmic concentration. These data suggest that the amount
285 of Rvs that is recruited scales with available concentration of protein. Comparing across ploidy
286 however, the rate of Rvs recruitment is lower in WT diploid compared to WT haploid (2xd vs 1xh,
287 Fig.4.1)

288 for this is not clear. 4.2 Arrangement of Rvs dimers on the membrane A homology model of
289 the Rvs BAR dimer structure based on Am-phiphysin suggests that it has the concave structure
290 typical for N-BAR domains. Rvs is a hetero- rather than homodimer unlike Am-phiphysin, and a
291 high-resolution structure will be necessary to clarify the interaction and arrangement of Rvs on
292 endocytic tubes. There are some indications from the experiments in this thesis however, regarding
293 its interaction with the membrane. 4.2.1 Rvs does not form a tight scaffold on membrane tubes
294 Observations of *in vitro* helices of BAR domains have suggested that Rvs might form a similar helical
295 scaffold. The number of Rvs molecules recruited to endocytic sites is high enough to cover the
296 surface area of the tubular invagination, so it has been proposed that an Rvs scaffold covers the
297 entire membrane tube up to the base of the future vesicle (Picco et al., 2015). In Rvs duplicated
298 diploid cells (4xd), Rvs can be recruited at a much faster rate than in the WT (2xd) (Fig.3.10B-
299 C, Fig.4.2) while disassembly dynamics is the same in both (Fig.3.10C, Fig.4.3). The exponential
300 decay of fluorescent intensity in WT haploid and diploid cells (1xh, 2xd, Fig.4.3) indicates that
301 all of the protein is suddenly disassembled from the endocytic site. When the membrane tube
302 undergoes scission, there is no more tubular curvature for the Rvs to bind to. The sharp decay is
303 therefore consistent with a BAR scaffold that breaks upon vesicle scission because there is no more
304 membrane interaction, releasing all the membrane-bound protein at once. A similar decay in the
305 4xd strain suggests that all the Rvs in this case is also bound to the membrane: if the protein was
306 not bound to the membrane, fluorescent intensity would not decay sharply. Since the membrane is
307 able to accommodate 1.4x the amount of BAR protein as the WT, it would suggest that at lower
308 protein amounts, a tight helix that covers the entire tube is not likely. Adding molecules to a tube
309 already completely covered by a scaffold would result in a change in Rvs assembly and disassembly
310 dynamics. Further, additional molecules would have to be added at the top or base of a tight
311 scaffold. At the top, the radius of curvature is decreased compared to the tube since this is the
312 rounded vesicle region. At the base, the plasma membrane is nearly flat, and the Rvs BAR domain
313 is similarly unlikely to favour interactions here. Otherwise the scaffold would have to be disrupted
314 to add new molecules, which would likely slow down recruitment rate rather than speed it up.
315 Molecules could also be added concentric to an existing scaffold. However, the concave surface of
316 Rvs is known to interact with lipids, and multiple layers of BAR domains on the membrane tube

317 would probably not show the sudden disassembly seen here. I assume that the membrane surface
318 area does not change in the 4xd compared to 2xd from the identical movement of Sla1 in both
319 cases (Fig.3.10A). It is possible that a wider tube is formed, which would increase the membrane
320 surface area for BAR binding. This would, however, require the BAR domains to interact with a lower
321 radius of curvature than in WT. This seems unlikely, and in the absence of any indication otherwise,
322 I assume that the membrane tubes in all diploid and haploid cases have the same width. 4.2.2 A
323 limit for how much Rvs can be recruited to the membrane In the case of Rvs duplication in haploids
324 (2xh), a change in disassembly dynamics is seen (Fig.3.9C, Fig.4.3). In 2xh, the maximum number
325 of molecules recruited is 178 ± 7.5 compared to the maximum of 113.505 ± 5.2 in WT (1xh). This is
326 means that nearly 1.6x the WT amount of protein is recruited to membrane tubes in the 2xh case.
327 The Rvs167 fluorescent intensity in 2xh shows a delay in disassembly. This suggests that the excess
328 protein may not be directly on the membrane, since if the protein was membrane bound, when the
329 membrane breaks, the protein must be released. The excess Rvs could either interact with the actin
330 network via the SH3 domain, or interact with other Rvs dimers. By a similar argument as in 4.2.1
331 above, I do not expect that multiple layers of BAR domains are formed, and that the excess protein
332 is recruited by the interaction of the SH3 domain. Another explanation for the delayed disassembly
333 is that at high concentrations of Rvs like in the 2xh case, a tight BAR scaffold is formed, and the
334 BAR domains interact with adjacent BAR domains. When the membrane undergoes scission, the
335 protein is no longer membrane-bound, but lateral interactions delay disassembly of the scaffold.
336 Lateral interactions between neighbouring BAR dimers have been shown in the case of Endophilin
337 (Mim et al., 2012). It is not currently clear where the Rvs molecules are added in the 2xh case:
338 superresolution microscopy could clarify whether it is added at the membrane tube. Whatever
339 the arrangement of the Rvs complex on the membrane, disassembly dynamics is changed in the
340 case of 2xh, compared to the other haploid and diploid strains. Since the number of Rvs molecules
341 is highest in this strain, this suggests that there is a limit to how much Rvs can assemble on the
342 tube without altering interaction with the endocytic protein network. 4.2.3 Conclusions for Rvs
343 localization All of these data support the idea that Rvs recruitment rate and total numbers are
344 determined by concentration of protein in the cell. The maximum number of molecules that can
345 interact with the membrane is limited by the surface area of the invagination. Although more can
346 be recruited, Rvs molecules over a certain threshold interact in a different way with endocytic sites,
347 possibly via the SH3 domain. Timing of recruitment to sites is by curvature-recognition via the BAR
348 domain, while efficiency of recruitment and interaction with the actin network is established via the
349 SH3 domain. 4.3 What causes membrane scission?

350 **Rvs acts as a membrane scaffold preventing membrane scission**

351 Invaginations in *rvs167Δ* cells undergo scission at short invagination lengths of about 80nm (Fig.3.2),
352 compared to the WT lengths of 140nm. This shows that first, enough forces are generated at
353 80nm to cause scission. Then, that Rvs167 is required at membrane tubes to prevent premature
354 scission. Prevention of scission at short invagination lengths can be explained by Rvs stabilizing
355 the membrane invagination via membrane interactions of the BAR domain (Boucrot et al., 2012;
356 Dmitrieff and Nedelec, 2015). Rvs preventing membrane scission could also be explained by the
357 SH3 domain mediating actin forces to the invagination neck: one can imagine that the SH3 domain
358 somehow decouples actin forces from the neck, and that this delays scission. Since invagination
359 lengths of *rvs167a* cells are increased towards WT by overexpression of the BAR domain alone
360 (Fig.3.12A), I propose that localization of Rvs BAR domains to the membrane tube stabilizes the
361 membrane. This allows deep invaginations to grow until actin polymerization produces enough
362 forces to overcome this stabilization and sever the membrane. Stabilization of the membrane
363 tube increases with increasing amounts of BAR domains recruited to the membrane tube (Fig.3.12).
364 The requirement for Rvs scaffolding cannot be removed by reducing turgor pressure (Fig.3.13),
365 suggesting that the function of the scaffold is not to counter turgor pressure.

366

367 Scission efficiency decreases with decreased amounts of Rvs: in diploids, lowering the amount
368 of Rvs by 20 molecules decreases scission efficiency to about 90% from 97%. This indicates that
369 a particular coverage of the membrane tube is required for effective scaffolding by BAR domains.
370 In support of this, in BAR strains, fewer numbers of Rvs are recruited, and scission efficiency is
371 similarly reduced. At low concentrations of Rvs like in the 1xd cells, it is likely that some membrane
372 tubes recruit the critical number of Rvs, in which case the invaginations grow to near WT lengths.
373 Over a certain amount of Rvs, adding more BAR domains does not increase the stability of the
374 tube: in 4xd, the same amount of actin is recruited before scission as in the 2xd and 1xd strains. If
375 enough forces are generated at 80nm, why is scission efficiency decreased in *rvs167Δ* compared
376 to WT? Forces from actin may be at a threshold when the invagination is at 80nm. There could be
377 enough force to sever the membrane, but not enough to sever reliably. The Rvs scaffold then keeps
378 the network growing to accumulate enough actin to reliably cause scission. Controlling membrane
379 tube length could also be a way for the cell to control the size of the vesicles formed, and therefore
380 the amount of cargo packed into the vesicle.

381 **What causes membrane scission?**

382 We have tested several scission models that include a major role for the Rvs complex. The seemingly
383 obvious solution to the scission problem is the action of a dynamin-like GTPase. If loss of the yeast
384 Dynamin Vps1 prevented or delayed scission, the membrane would continue to invaginate longer
385 than WT lengths, and Sla1 movements of over 140nm should be observed. Rvs centroid movement
386 would likely also be affected: a bigger jump inwards could indicate that a longer membrane has
387 been cut. That neither is seen in the behaviour of coat and scission markers indicates that even if
388 Vps1 is recruited to endocytic sites, it is not necessary for Rvs localization or function, and is not
389 necessary for scission. The Inp51, Inp52 data tests the lipid hydrolysis model, in which synaptojanins
390 hydrolyze PIP2 molecules that are not covered by BAR domains, resulting in a boundary between
391 hydrolyzed and non- hydrolyzed PIP2. This model predicts that interfacial forces generated at the
392 lipid boundary causes scission (Liu et al., 2006). Inp51 is not seen in patches at the cellular cortex,
393 but this could be because protein recruitment is below our detection threshold. Inp52 localizes to
394 the top of invaginations right before scission, consistent with a role in vesicle formation (Fig.3.7D).
395 Some predictions of the lipid hydrolysis model are inconsistent with our data, however. First, vesicle
396 scission is expected to occur at the interphase of the hydrolyzed and non-hydrolyzed lipid. Since the
397 BAR scaffold covers the membrane tube, this interphase would be at the top of the area covered by
398 Rvs. Kukulski et al., 2012 have shown that vesicles undergo scission at 1/3 the invagination length
399 from the base: that is, vesicles generated by the lipid boundary would be smaller than have been
400 measured. Second, removing forces generated by lipid hydrolysis by deleting synaptojanins should
401 increase invagination lengths, since scission would be delayed or it would fail without those forces.
402 Deletion of neither Inp51 nor Inp52 changes the invagination lengths: Sla1 movement does not
403 increase. That the position of the vesicle formed is also unchanged compared to WT is indicated by
404 the similar magnitude of the jump into the cytoplasm of the Rvs centroid. There are some changes
405 in the synaptojanin deletion strains (Fig.3.8). In *inp51Δ* cells, Rvs assembly is slightly slower than
406 that in WT. Therefore, Inp51 could play a role in Rvs recruitment. In the *inp52Δ* strain, about 12% of
407 Sla1-GFP tracks retract, indicated that scission fails in those cases. Although this is low compared to
408 the failed scission rate of *rvs167Δ* cells (close to 30%), this data could suggest a moderate influence
409 of Inp52 on scission. Rvs centroid persists after scission for about a second longer in *inp52Δ* cells
410 than in WT, indicating that disassembly of Rvs on the base of the newly formed vesicle is delayed.
411 Inp52 is likely involved in vesicle un- coating. Deletion of synaptojanin-like Inp52 does not affect the
412 movement of the invagination. In spite of this, Sla1 patches persist for longer after scission in the
413 *inp52Δ* than in WT cells, as does Rvs167, indicated by the arrows in Fig.3.8A,D. Persistence of both
414 suggests that rather than the scission timepoint, post-scission disassembly of proteins from the
415 vesicle is inhibited in *inp52Δ* cells. Inp52 then plays a role in recycling endocytic proteins from the
416 vesicle to the plasma membrane. The slower assembly of Rvs in *inp51Δ* and the increase in coat

417 retraction rates of *inp52Δ* could indicate that there is a slight effect on Rvs recruitment, and that
418 lipid hydrolysis could play a small role in scission.

419
420 Protein-friction mediated membrane scission proposes that BAR domains induce a frictional force
421 on the membrane, causing scission. In Rvs duplicated haploid cells (2xh), adding up to 1.6x the
422 WT (1xh) amount of Rvs to membrane tubes does not affect the length at which the membrane
423 undergoes scission (Fig.3.9). If more BAR domains were added to the membrane tube, frictional
424 force generated as the membrane is pulled under it should increase, and the membrane should
425 rupture faster. That is, membrane scission occurs as soon as WT forces are generated on the tube.
426 Since BAR domains are added at a faster rate in the 2xh cells, these forces would be reached at
427 shorter invagination lengths. In 2xh cells, WT amount of Rvs is recruited at about 1.8 seconds before
428 maximum fluorescent intensity, but scission does not occur at this time. Instead, Rvs continues
429 to accumulate, and the invagination continues to grow. In diploid strains, adding 1.4x the WT
430 amount of Rvs in the 4x Rvs case also does not change length of membrane that undergoes scission.
431 Therefore, protein friction due to Rvs does not appear to contribute significantly to membrane
432 scission in yeast endocytosis.

433 Maximum amount of Abp1 measured in all the diploid strains is about 220 molecules (Fig.3.11).
434 In this case, only one allele of Abp1 is fluorescently tagged, so half the amount of Abp1 recruited
435 is measured. The maximum amount of Abp1 recruited is then double that measured, which is
436 about 440 ± 20 molecules (assuming equal expression and recruitment of tagged and untagged
437 Abp1). In WT haploid cells, the maximum number of Abp1 measured is 460 ± 20 molecules. That the
438 same number of molecules of Abp1 is recruited in all cases before scission indicates that scission
439 timing depends on the amount of Abp1, and hence, on the amount of actin recruited. This data
440 is consistent with actin supplying the forces necessary for membrane scission. The membrane
441 invagination continues until the "right" amount of actin is recruited. At this amount of actin, enough
442 forces are generated to rupture the membrane. The amount of force necessary is determined by
443 the physical properties of the membrane like membrane rigidity, tension, and proteins accumulated
444 on the membrane (Dmitrieff and Nedelec, 2015). Vesicle scission releases membrane-bound Rvs,
445 resulting in release of the SH3 along with BAR domains. Release of the SH3 domains could indicate
446 to its binding partner in the actin network that vesicle scission has occurred, beginning disassembly
447 of actin components. In BAR strains, a low amount of actin is recruited (Fig.3.4C). Although the
448 absence of the SH3 domain severely perturbs the actin network, the mechanistic effect of this
449 perturbation is unclear.

450 **Model for membrane scission**

451 I propose that Rvs is recruited to sites by two distinct mechanisms. SH3 domains cluster Rvs
452 at endocytic sites. This SH3 interaction increases the efficiency with which the BAR domains
453 sense curvature on tubular membranes. BAR domains bind to endocytic sites by sensing tubular
454 membrane. BAR domains are recruited over the entire membrane tube, but do not form a tight
455 helical scaffold. Membrane shape is stabilized against fluctuations that could cause scission by
456 the BAR-membrane interaction. This prevent actin forces from rupturing the membrane, and the
457 invaginations continue to grow in length as actin continues to polymerize. BAR recruitment to
458 membrane tubes is restricted by the surface area of the tube: after a certain amount of Rvs, the
459 excess interacts with endocytic sites via the SH3 domain. Adding over a certain amount of Rvs also
460 does not increase the stabilization effect on the tube. As actin continues to polymerize, at a certain
461 amount of actin, enough forces are generated to overcome the resistance to membrane scission
462 provided by the BAR scaffold. The membrane ruptures, and vesicles are formed. Synaptojanins
463 may help recruit Rvs at endocytic sites: Inp51 and Inp52 have proline rich regions that could act as
464 binding sites for Rvs167 SH3 domains. They are involved in vesicle uncoating post-scission, likely by
465 dephosphorylating PIP2 and inducing disassembly of PIP2-binding endocytic proteins. Eventually
466 phosphorylation regulation allows endocytic proteins to be reused at endocytic sites, while the

467 vesicle is transported elsewhere into the cell.
468 Morbi luctus, wisi viverra faucibus pretium, nibh est placerat odio, nec commodo wisi enim eget
469 quam. Quisque libero justo, consectetur a, feugiat vitae, porttitor eu, libero. Suspendisse sed
470 mauris vitae elit sollicitudin malesuada. Maecenas ultricies eros sit amet ante. Ut venenatis velit.
471 Maecenas sed mi eget dui varius euismod. Phasellus aliquet volutpat odio. Vestibulum ante ipsum
472 primis in faucibus orci luctus et ultrices posuere cubilia Curae; Pellentesque sit amet pede ac sem
473 eleifend consectetur. Nullam elementum, urna vel imperdiet sodales, elit ipsum pharetra ligula,
474 ac pretium ante justo a nulla. Curabitur tristique arcu eu metus. Vestibulum lectus. Proin mauris.
475 Proin eu nunc eu urna hendrerit faucibus. Aliquam auctor, pede consequat laoreet varius, eros
476 tellus scelerisque quam, pellentesque hendrerit ipsum dolor sed augue. Nulla nec lacus.

477 **Methods and Materials**

478 Guidelines can be included for standard research article sections, such as this one.
479 Nulla malesuada porttitor diam. Donec felis erat, congue non, volutpat at, tincidunt tristique,
480 libero. Vivamus viverra fermentum felis. Donec nonummy pellentesque ante. Phasellus adipiscing
481 semper elit. Proin fermentum massa ac quam. Sed diam turpis, molestie vitae, placerat a, molestie
482 nec, leo. Maecenas lacinia. Nam ipsum ligula, eleifend at, accumsan nec, suscipit a, ipsum.
483 Morbi blandit ligula feugiat magna. Nunc eleifend consequat lorem. Sed lacinia nulla vitae enim.
484 Pellentesque tincidunt purus vel magna. Integer non enim. Praesent euismod nunc eu purus.
485 Donec bibendum quam in tellus. Nullam cursus pulvinar lectus. Donec et mi. Nam vulputate metus
486 eu enim. Vestibulum pellentesque felis eu massa.

487 **Citations**

488 LaTeX formats citations and references automatically using the bibliography records in your .bib
489 file, which you can edit via the project menu. Use the \cite command for an inline citation, like
490 ?, and the \citep command for a citation in parentheses (?). The LaTeX template uses a slightly-
491 modified Vancouver bibliography style. If your manuscript is accepted, the eLife production team
492 will re-format the references into the final published form. *It is not necessary to attempt to format*
493 *the reference list yourself to mirror the final published form.* Please also remember to **delete the line**
494 \nocite{*} in the template just before \bibliography{...}; otherwise *all* entries from your .bib
495 file will be listed!

496 **Acknowledgments**

497 Additional information can be given in the template, such as to not include funder information in
498 the acknowledgments section.